INTERNATIONAL JOURNAL OF
COASTAL, OFFSHORE & ENVIRONMENTAL ENGINEERING IJCOE Vol.9/No. 4/Autumn 2024 (20-29)

Available online at: www. Ijcoe.org

Numerical simulation of flow for improved width of the shipwreck in the curvature of the Waal River in Netherlands by using of Groyns

Parisa Alinouri [1], Mehdi Nezhadnaderi[2]*, Mohammad Hossein Vafaee [3], Babak Fazli Malidareh[4], Babak Pordel Maragheh[5]

[1)] MSc of Water Engineering- Water Structures, Imam Khomeini International University, Qazvin, Iran. P.alinouri2018@gmail.com
*[*2)] Department of Civil Engineering, Tonekabon Branch, Islamic Azad University, Tonekabon, Iran. (Corresponding Author). mehdi2930@yahoo.com.*
[3)] Assistant Professor, Department of Civil Engineering, Pooyesh Instituteof Higher Education, Qom.Iran. M.h.vafaee2024@gmail.com
[4)] Department of Civil Engineering, Babol Branch, Islamic Azad University, Babol, Iran. Fazli.babak@babolia.ac.ir
[5)] Department of Civil Engineering, Ardabil Branch, Islamic Azad University, Ardabil, Iran. civil_babak2005@yahoo.com

ARTICLE INFO

Article History:
Received: 1 Aug 2024
Accepted: 15 Oct 2024

Keywords:
Groyne,
Flow pattern
Secondary currents
90 Degree bend
Waal river

ABSTRACT

One of the effective methods for protecting the shores of navigable rivers at the site of the arches is the use of groynes. In order to study a case in the Netherlands, a numerical study was carried out on the effects of using submerged vanes with vertical groynes on the protection of the Waal coast in Netherlands. In the present study, the numerical results of the impact of vertical groynes series with 5 angular deviations were compared to the external arc wall with a length of 25% channel width (87.5 m) and a spacing of 595.859 meters with a nonsubmerged vane at a distance of one fourth of the width of the internal arc with a full arc length of 90 degrees are paid to the average velocity distribution and pressure in the arc of 90 degrees, with a width of 350 meters and a depth of 4.5 meters. The results of the study showed that the presence of groynes series causes uniformity of upstream velocity and high- velocity transmission from the inner arc to the middle of the canal. In the case of the presence of groynes in the outer arc with a submerged vane close to the inner arch, about one quarter of the width of the internal arc produces a counterflow stream that reduces the normal secondary flow in the bends of the river. Hence, the high- velocity current, which is driven radially to the inner shore, is diverted to the middle direction. So it will improve the sedimentation on the inner shore of the bend and scouring on the outer

1) MSc
2) Associate Professor
3) Assistant Professor

shore of the bend. In this way, the flow rate from the mean value of one meter per second reaches 1.98 m/s in the middle region and decreases from the sedimentation in this range.

1. Introduction

With the increase of construction on the banks of the rivers, the use of protective structures to preserve and restore the banks of the rivers is considered. Among the coastal protection structures, there are breakwaters that are used in coastal engineering to protect and stabilize beaches. These structures are simple in terms of structure and have the ability to adapt to all kinds of diverse conditions and have a wide application in stabilization and stabilization of beaches, hence the investigation and understanding of the process of erosion and sedimentation in the area of breakwaters in terms of design, protection and maintenance are very important.

Considering that the topic of this research is related to the effect of using breakwaters in coastal protection, it is appropriate to briefly describe the organization methods and determine the position of breakwaters before entering the main discussion and dealing with it. Considering that in many cases, the design and construction of breakwaters is not cost-effective due to the lack of access to suitable materials, although breakwaters have been used in different cases in different countries, but the criteria and design criteria for it are not clear. Because these types of structures can be used in many cases to protect the coasts of the country, it seems necessary to study and research in this case.

In recent decades, many laboratory or numerical studies have been conducted in the field of flow patterns in arches, which led to the development of different methods and techniques for river management, among which the laboratory study of Shukri (1950) can be mentioned. He observed that for an arc with a gentle curve, the place of maximum velocity in the first half of the arc inclines towards the inner wall and moves towards the exit of the arch towards the outer wall. Based on the research of Vashni and Grade (1975) when R/B (ratio).

If the radius of the arch is more than 3.5, the shear stress distribution in the entrance section of the arch is almost uniform, and the maximum stress area occurs in the exit part of the arch and its outer wall (cited by Ghodisian, 2008).

Tingsanchali and Maheswaran (1990) used a two-dimensional numerical model to investigate the distribution of average velocity and bed shear stress near a breakwater located in a rectangular channel, and according to the curvature of the flow lines around the breakwater, they added a correction factor to the k-ε model.

Giri et al. (2004) investigated the flow and turbulence pattern in a flume similar to spiral rivers by changing the position of the non-submersible breakwaters investigated its effect on the flow field around the breakwater. The results of the experiments and their comparison with the extended model showed the effectiveness of the above model in showing the distribution of the speed and intensity of the flow in the shear layer.

2008) used measured three-dimensional velocity data in small agricultural waterways in the Midwest region to determine the flow pattern around submerged weirs constructed in the arch of the waterway. These researchers developed a three-dimensional mathematical model to simulate the flow pattern around submerged spillways and used real data to calibrate their model.

Duan et al. (2009) obtained three-dimensional data of velocity in a straight channel with the presence of a rectangular breakwater and investigated the flow pattern in two flow fields of smooth bottom and bottom with scour hole. Their research shows an increase in the longitudinal and transverse components and a decrease in the vertical component of the velocity after the formation of the scour hole, and the shear stress of the bed around the scour is reported to be six to eight times greater than the upstream shear stress.

Van den Hewer - (2013) conducted a laboratory study to investigate the erosion, sedimentation and flow hydraulics in a laboratory model made similar to spiral rivers. The length, distance and placement angle of breakwaters were the variables studied by him. From the results of his research, we can refer to the report of the creation of a low-velocity area between breakwaters, where sedimentation takes place in this area. As the distance between the breakwaters increases, the speed between the breakwaters increases, and this increase in speed causes a change in the sedimentation pattern between the breakwaters.

Qodsian et al. (2007) investigated the two-dimensional flow pattern around a single breakwater in different positions in the arch and with changes in the length of the breakwater and the descent number of the flow, from the results of this research, the ratio of the maximum shear stress to the upstream shear stress at the breakwater location and to the maximum It reaches 10 to 20 degrees downstream of the breakwater.

Fazli et al. (2008) conducted a research and compared the shear stress calculation methods in arched channels. In this laboratory research, computational stresses were investigated and compared with two methods of averaging velocity in depth and using Reynolds stress. The results of this research showed that the distribution of shear stress in the arch, which is obtained by averaging in depth, is more consistent with the process of scouring and deposition in the arch than the distribution of shear stress calculated by the method of Reynolds stresses. Also, how The distribution of the average velocity of the flow near the bottom, which is related to the shear stress of the bed, shows better agreement with the shear stress calculated by the averaged velocity method in depth. Qodsian (2008) investigated the effect of different parameters on the flow and scour pattern around the breakwater in the 90 degree arc. Among these parameters, we can mention the flow rate, the length of the breakwater, the location of the breakwater in the arch, the distance and number of breakwaters, and the radius of curvature of the arch. From the results of this research, it can be pointed out that the amount of shear stress upstream of a single breakwater does not change with the increase in its length and the increase in shear stress at the breakwater location with the increase in the length of the breakwater. Also, the results of this research show the deviation of the high-speed area from the vicinity of the outer wall of the arch towards the inner wall and the middle of the channel by installing breakwaters in different positions of the arch.

2. Methods

A critical review of available turbulence models with the aim of evaluating their suitability for use in hydraulic problems is valuable and needed. This was done by Professor Wolfgang Reddy with years of experience in the development and application of these models. In the book ((turbulence models and their application in hydraulics)), he introduced the topic of turbulence modeling in a simple way that can be understood by any reader with basic knowledge in the field of fluid mechanics and summarized the latest published articles in this field. is In the first chapter, the role of turbulence models is explained (Salehi Nishabouri and Nasiri Saleh, 2017).

Basic conservation laws are expressed by exact equations (Navier-Stokes equations). They describe all the details of fluid movement. Since there is little hope to solve these equations and also due to the lack of interest of engineers in the details of oscillatory motion, a statistical approximation (which was first proposed by Asburn Reynolds) was used and these equations, on the time scale - which in The comparison with the time scale of turbulent motion is large - they were averaged.

Unfortunately, the averaging operation creates a new problem that the equations cannot form a closed system, because they contain unknown sentences that describe the transfer of the amount of motion, heat, and average mass by means of turbulent motion. This system of equations can be closed only by using experimental input, therefore, calculation methods based on averaged flow equations are semi-empirical.

The so-called field methods - which use the original partial differential equations - require the specifications of the turbulent transfer terms that appear in the equations at every point of the flow. This specification is defined by using the equations (algebraic or differential) that determine the turbulent transfer terms in the average flow equations, and the system of equations is closed using those equations. The basis of chaos models are hypotheses about chaotic processes that require experimental input in the form of constants or functions. They do not simulate the details of the turbulent motion, but simply "simulate the effect of turbulence on the behavior of the average flow" (Salehi Nishabouri and Nasiri Saleh, 2017).

In this study, flow is unsteady with two-dimensional turbulence form. Velocity and pressure are a function of time and space. To model of the velocity and pressure fluctuations is the integrated from the Navier Stokes equation at time. Integration of Navier Stokes equations at time is known Reynolds equations (Reynolds, 1984). Turbulence model equations are two equation models k-ε (Standard) that have be averaged in depth (Rastogi and Reddy, 1978). ε equation is as one of the main sources of the limitations of accuracy of the standard version of the k-ε model and the Reynolds stress model. It is interesting that k-ε model includes a correction term that is dependent to strain with c13 constant in the ε equation of RNG model (Yakhot et al, 1992). WillCox provided turbulence equations of k-ω (standard) model (WillCox, 1988).

$$\frac{\partial u}{\partial x} + \frac{\partial v}{\partial y} + \frac{\partial w}{\partial z} = 0 \qquad (1)$$

$$\frac{\partial \rho u}{\partial t}+\frac{\partial \rho uu}{\partial x}+\frac{\partial \rho uv}{\partial y}+\frac{\partial \rho uw}{\partial z}-\rho f_c v=-\frac{\partial P}{\partial x}+\frac{\partial \tau_{xx}}{\partial x}+\frac{\partial \tau_{xy}}{\partial y}+\frac{\partial \tau_{xz}}{\partial z} \quad (2)$$

$$\frac{\partial \rho v}{\partial t}+\frac{\partial \rho uv}{\partial x}+\frac{\partial \rho vv}{\partial y}+\frac{\partial \rho vw}{\partial z}+\rho f_c u=-\frac{\partial P}{\partial y}+\frac{\partial \tau_{yx}}{\partial x}+\frac{\partial \tau_{yy}}{\partial y}+\frac{\partial \tau_{yz}}{\partial z} \quad (3)$$

$$\frac{\partial \rho w}{\partial t}+\frac{\partial \rho uw}{\partial x}+\frac{\partial \rho vw}{\partial y}+\frac{\partial \rho ww}{\partial z}=-\frac{\partial P}{\partial z}+\frac{\partial \tau_{zx}}{\partial x}+\frac{\partial \tau_{zy}}{\partial y}+\frac{\partial \tau_{zz}}{\partial z}-\rho g \quad (4)$$

Turbulence model equation

Known two-equation model of k-ε (Standard) are presented for averaged form in depth as follows: (Rastogi and Reddy, 1978).

$$\frac{\partial hk}{\partial t}+\frac{\partial U_j hk}{\partial x_j}=\frac{\partial}{\partial x_j}[(\nu+\frac{\nu_t}{\sigma_k})h\frac{\partial k}{\partial x}]+hP_k+hP_{kv}-h\varepsilon \quad (5)$$

$$\frac{\partial h\varepsilon}{\partial t}+\frac{\partial U_j h\varepsilon}{\partial x_j}=\frac{\partial}{\partial x_j}[(\nu+\frac{\nu_t}{\sigma\varepsilon})h\frac{\partial \varepsilon}{\partial x}]+hc_{1\varepsilon}\frac{\varepsilon}{k}P_k+hP_{\varepsilon v}-hc_{2\varepsilon}\frac{\varepsilon^2}{k} \quad (6)$$

$$\frac{\partial h\varepsilon}{\partial t}+\frac{\partial U_j h\varepsilon}{\partial x_j}=\frac{\partial}{\partial x_j}\left[\left(\nu+\frac{\nu_t}{\sigma_\varepsilon}\right)h\frac{\partial \varepsilon}{\partial x}\right]+hc_{1\varepsilon}\frac{\varepsilon}{k}P_k+hP_{\varepsilon v}-hc_{2\varepsilon}\frac{\varepsilon^2}{k}\ \nu_t=c_\mu\frac{k^2}{\varepsilon},P_k=2\nu_t S_{ij}.S_{ij} \quad (7)$$

$$P_{kv}=c_k\frac{k^2}{\varepsilon},c_k=\frac{1}{c_f^{1/2}},P_{\varepsilon v}=c_\varepsilon\frac{u_f^4}{h^2},c_\varepsilon=\frac{1}{\sqrt{e_*\sigma_t}}\frac{c_{2\varepsilon}c_\mu^{1/2}}{c_f^{3/4}},c_f=\frac{u_f^2}{u^2+v^2+w^2}=\frac{n^2g}{h^{1/3}} \quad (8)$$

$$c_\mu=0.09,c_{\varepsilon 1}=1.44,c_{\varepsilon 2}=1.92,\sigma_k=1.0,\sigma_\varepsilon=1.31$$

P_{kv} and P_{kv} are production terms as result of non-uniform distribution velocity in depth that is stronger near-bed. P_k is production term of turbulent kinetic energy averaged in depth as result of velocity gradients in the plan. ν_t is the vortex viscosity. Turbulence model is used for calculation of lateral flow into one channel and is achieved much better results in comparison with ν_t for fixed parameters of rotational flow (MCGurik and Rodi, 1978). c_f is the bed friction coefficient. σ_t is Schmidt number that shows relationship between turbulence viscosity and turbulent diffusion coefficient according to the following equation:

$$\varepsilon_d=\frac{\nu_t}{\sigma_t} \quad (9)$$

Amount of σ_t is considered 0.5 (Keller and Rodi, 1988). Although values of σ_t are 0.5 to 2 in variable references (Gibson and launder, 1978). e_* is coefficient that gives turbulence diffusion coefficient in depth by following equation (Keller and Rodi, 1988).

$$\varepsilon_d=e_* hu_f \quad (10)$$

Direct measurement of color broadcasting in the fixed-width channels offers 0.15 for e_*. Although Keller and Rodi achieved better solutions for the velocity and stress within the composite channels (Keller and Rodi, 1988). On the other hand Biglari and Sturm have been assumed e_* equaled to 0.3 to get the better answer within the composite channels (Biglari and Sturm, 1998). MCGurik and Rodi have considered $\frac{1}{\sqrt{e_*\sigma_t}}$ equaled to 3.6 (MCGurik and Rodi, 1978). In ε equation of RNG model includes a correction term $c_{\varepsilon 1}$ that is constant strain-dependent (Yakhot et al, 1992). For k-ε (RNG), we have:

$$\frac{\partial h\varepsilon}{\partial t}+\frac{\partial U_j h\varepsilon}{\partial x_j}=\frac{\partial}{\partial x_j}[(\nu+\frac{\nu_t}{\sigma\varepsilon})h\frac{\partial \varepsilon}{\partial x}]+hc_{1\varepsilon}^*\frac{\varepsilon}{k}P_k+hP_{\varepsilon v}-hc_{2\varepsilon}\frac{\varepsilon^2}{k} \quad (11)$$

$$c_\mu=0.0845,c_{1\varepsilon}^*=c_{1\varepsilon}-\frac{\eta(1-\frac{\eta}{\eta_0})}{1+\beta\eta^3},c_{1\varepsilon}=1.68,\sigma_k=1.39,\beta=0.0$$

$$\eta=(2E_{ij}.E_{ij})^{1/2}\frac{k}{\varepsilon},\eta_0=4.377 \quad (12)$$

Only constant β is adjustable, high levels of turbulent data are obtained near-wall. All other constants are calculated explicitly as part of the RNG process.

$$\frac{\partial hk}{\partial t}+\frac{\partial U_j hk}{\partial x_j}=\frac{\partial}{\partial x_j}[(\nu+\frac{\nu_t}{\sigma_k})h\frac{\partial k}{\partial x}]+P_k+P_b-h\varepsilon \quad (13)$$

$$\frac{\partial h\varepsilon}{\partial t}+\frac{\partial U_j h\varepsilon}{\partial x_j}=\frac{\partial}{\partial x_j}[(\nu+\frac{\nu_t}{\sigma\varepsilon})h\frac{\partial\varepsilon}{\partial x}]+hc_{1\varepsilon}\frac{\varepsilon}{k}P_k+hc_1S_\varepsilon-hc_2\frac{\varepsilon^2}{k+\sqrt{\nu\varepsilon}}+S_\varepsilon \quad (14)$$

$$c_1=Max[0.43,\frac{\eta}{\eta+s}],\eta=s\frac{k}{\varepsilon},s=\sqrt{2s_{ij}s_{ij}},\mu_t=hc_\mu\frac{k^2}{\varepsilon},P_k=-\rho\overline{u_i^{'}u_j^{'}}\frac{\partial u_j}{\partial x_i^{'}},$$

$$P_k=\mu_t s^2,P_b=\beta g_i\frac{\mu_t}{\Pr_t}\frac{\partial T}{\partial x_i},\mu_t=\rho c_\mu\frac{k^2}{\varepsilon},c_\mu=\frac{1}{A_0+A_s\frac{KU^*}{\varepsilon}},U^*=\sqrt{s_{ij}s_{ij}+\overline{\Omega_{ij}}\,\overline{\Omega_{ij}}}, \quad (15)$$

$$\overline{\Omega_{ij}}=\Omega_{ij}-\varepsilon_{ijk}\omega_k,A_0=4.04,A_s=\sqrt{6}\cos\Phi,\Phi=\frac{1}{3}\cos^{-1}(\sqrt{6}\omega),\omega=\frac{s_{ij}s_{jk}s_{ki}}{\tilde{s}^3},\tilde{s}=\sqrt{s_{ij}s_{ij}},$$

$$s_{ij}=\frac{1}{2}(\frac{\partial u_j}{\partial x_i}+\frac{\partial u_i}{\partial x_j}),c_{1\varepsilon}=1.44,c_2=1.9,\sigma_k=1,\sigma_\varepsilon=1.2,\beta=-\frac{1}{\rho}(\frac{\partial P}{\partial T})p,\Pr_t=0.85$$

WillCox, turbulence model k-ω (standard) equation to be provided as follows: (WillCox, 1988):

$$\frac{\partial k}{\partial t}+U_j\frac{\partial k}{\partial x_j}=\tau_{ij}\frac{\partial U_i}{\partial x_j}-\beta^*k\omega+\frac{\partial}{\partial x_j}[(\nu+\sigma^*\nu_T)\frac{\partial k}{\partial x_j}] \quad (16)$$

$$\frac{\partial\omega}{\partial t}+U_j\frac{\partial\omega}{\partial x_j}=\alpha\frac{\omega}{k}\tau_{ij}\frac{\partial U_i}{\partial x_j}-\beta\omega^2k\omega+\frac{\partial}{\partial x_j}[(\nu+\sigma\nu_T)\frac{\partial\omega}{\partial x_j}] \quad (17)$$

$$\frac{\partial k}{\partial t}+U_j\frac{\partial k}{\partial x_j}=\tau_{ij}\frac{\partial U_i}{\partial x_j}-\beta^*k\omega+\frac{\partial}{\partial x_j}[(\nu+\sigma^*\nu_T)\frac{\partial k}{\partial x_j}]$$

$$\nu_t=\frac{k}{\omega},\alpha=\frac{5}{9},\beta=\frac{3}{40},\beta^*=\frac{9}{100},\sigma=\frac{1}{2},\varepsilon=\beta^*\omega k$$

3. Numerical Model

The values of the physical properties of water are considered as a default respectively, for density, viscosity, heat capacity and thermal conductivity. Solutions of all governing equations are subject to assignment of variables correctly in the boundary nodes. In steady state problems required only boundary condition but in unsteady state problems is required the initial conditions for all nodes in the network. Common boundary conditions in hydraulic issues include (Soltani and Rahimi Asl, 2003):

A- Inlet boundary condition: numerical models can fit the model by means of the various boundary conditions such as velocity, mass flow, etc. For example, in modeling of flow inside a closed or open channel can be used velocity inlet as input boundary condition.

B- The outlet boundary condition is considered pressure outlet equals the atmospheric pressure. If the output is chosen at a far distance from geometric constraints, and no change in direction of flow then the flow state is developed full. Using this model is caused the output surface is perpendicular to the flow and gradient is zero in the perpendicular direction on the output surface (Soltani and Rahimi Asl, 2003).

C - Wall boundary condition: the wall boundary condition is used to limit the area of between fluid and solid. The model is ready for simulation by Solutions set and defining the model. The following steps show the simulation process (Versteeg and Malalasekera, 2007): selection methods of discretization equation: In this paper first order upstream difference method is used for discretization of momentum, k, ε and ω equations and the standard method is used to find the pressure. Selection methods of the relation velocity - Pressure: this step is only be studied segregated. In this paper is used from SIMPLE method for velocity - pressure coupling. Determine the discount factors: the discount factor values are used for control of calculated variables in the each iteration. In this paper, the default values are used respectively for the pressure, density, momentum, k, ε and turbulent viscosity. In this paper, the initial values of the relative pressure is considered zero And the initial values of velocity components close to the average values presented in the input stream. By completing the steps in the numerical model, we can start the introduced process of problem by defining of repeat process. The frequency of reporting of results can be introduced before computing the numerical model. During solution process can be seen convergence of solution by the control of residues, integral of surface, statistics and values of the force. After finishing solution the computation of the unknown quantities and the results can be calculated at any point of the field and can be displayed by vector in the form, contour and profile views (Versteeg and Malalasekera, 2007). In this paper for solution of flow is usually introduced initial number repeat 1000 with report of every step of the calculation that conditions for convergence of the unknown parameters were satisfied after 300 to 350 iterations.

The dimensions of the Waal river in the Netherlands are not sufficient for the development of inland waterways, so it must be enlarged to increase the shipping capacity. In the middle part of the Vaal river between Nijmegen and Tiel, the extension of the handles in long and straight spans is an option. But in the bends of the upstream and downstream areas of the river, due to the difference in morphological and

hydraulic processes (spiral flow), a different solution is needed. The Dutch Ministry of Public Works commissioned Haskoning to prepare a preliminary design to improve the width of the navigable part of the channel in one of the bends of the river through the use of submerged fins. Submerged fins are thin slabs or wing-shaped walls that are installed on the stream bed in a river. And they usually have an angle with the main flow direction. When placed at the optimal angle, submerged vanes produce an anti-helix flow that reduces, or even possibly completely eliminates, the natural secondary flow in river bends. This is why the sediment flow, which is originally pushed towards the inner bank of the bend, is changed and directed to the opposite side. Therefore, it will improve sedimentation on the outer shore of the bend and washing water on the inner shore of the bend.

Figure 1- Map of navigable rivers in the Netherlands and the location of the Waal river in it.

Figure 2- The picture of the Waal river and the vertical breakwater structures in the outer arch and the middle wall in its inner arch

In this research, version 16/3/2 of Gambit software is used to generate its geometry and grid. The grid pattern is made of Quad element and map type is used for pages. The available boundary conditions are the velocity input from the left side from the top of the arc and the pressure output boundary condition at the bottom of the arc. The simulation results can be seen in Figures 3 to ١١.

4. Results and Discussions

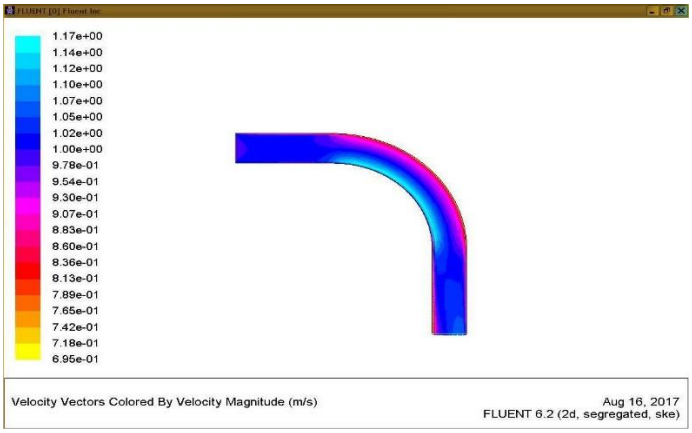

Figure 3- Velocity curve, meters per second, in a 90-degree arc with a width of 350 meters and a water height of 4.5 meters. K- ε perturbation model is used. The results show that the velocity values in the inner arc obtained from the numerical model in the state without the presence of coastal protection structures immediately after the end of the straight path of the channel and at the beginning of the inner arc equal to 1.17 m/s and in the outer arc equal to 8.13 meters per second.

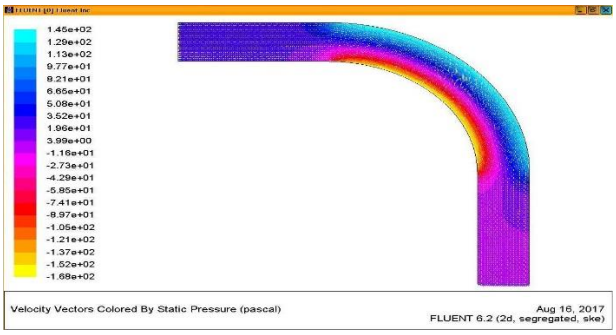

Figure 4- Isometric pressure curve in terms of pascal, in a 90 degree arc with a width of 350 meters and a water height of 4.5 meters. K- ε perturbation model is used. The results show that the amount of negative pressure in the inner arc obtained from the numerical model in the absence of coastal protection structures immediately after the end of the straight path of the channel and at the beginning of the inner arc equals -1.68e+2 pascal and the positive pressure in the outer arc equals It is 1.45e+2 pascal. In the inner arc, the sedimentation potential is higher and in the outer arc, due to the positive hydrostatic forces, the erosion potential is higher.

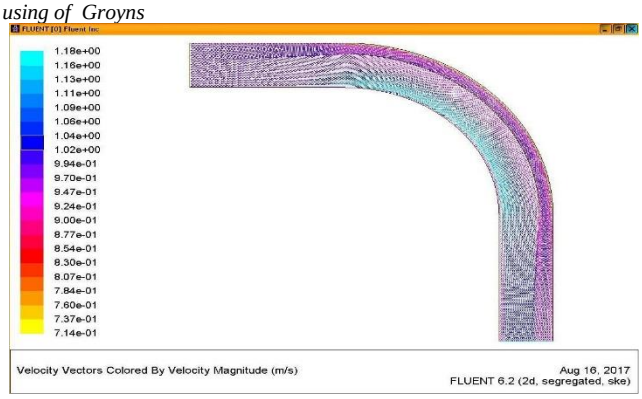

Figure 5- Isometric curve, meters per second, in a 90-degree arc with a width of 350 meters and a water height of 4.5 meters. K- ε perturbation model is used. The results show that the velocity values in the inner arc obtained from the numerical model in the presence of the arc vane in a quarter of the width near the outer arc of the coast immediately after the end of the straight path of the channel and at the beginning of the inner arc, equal to 1.18 m/s and in the arc External is equal to 8.77 meters per second. Compared to the state without this structure, there was not much change

.

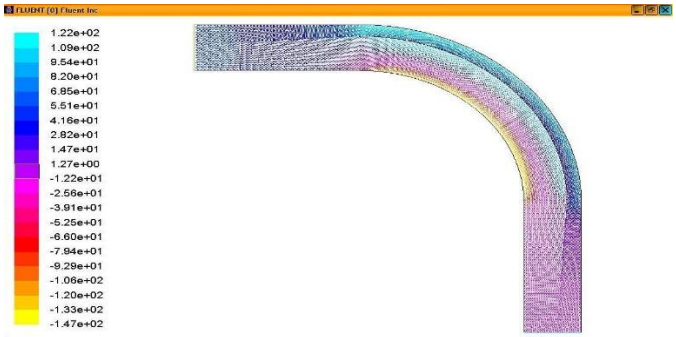

Figure 6- Isometric curve in terms of pascal, in a 90 degree arc with a width of 350 meters and a water height of 4.5 meters. K- ε perturbation model is used. The results show that the amount of negative pressure in the inner arch obtained from the numerical model in the presence of the arch vane in a quarter of the width near the outer arch of the coast immediately after the end of the straight path of the channel and at the beginning of the inner arch, is equal to -1.68e+2 pascal and the pressure Positive in the outer arc is equal to 1.45e+2 pascal. In the inner arc, the sedimentation potential is higher and in the outer arc, due to the positive hydrostatic forces, the erosion potential is higher. Compared to the state without this structure, there was not much change.

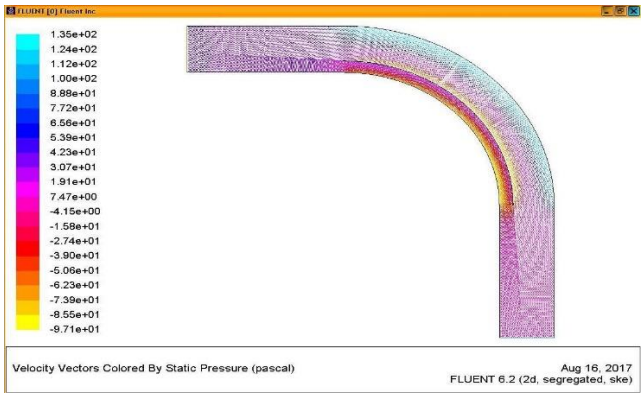

Figure٧ - Isometric curve in terms of pascal, in a 90 degree arc with a width of 350 meters and a water height of 4.5 meters. K- ε perturbation model is used. The results show that the amount of negative pressure in the inner arch obtained from the numerical model in the presence of the arch vane in a quarter of the width near the inner arch of the beaches immediately after the end of the straight path of the channel and at the beginning of the inner arch, is equal to -9.71e+1 pascal and the pressure Positive in the outer arc is equal to 1.355e+2 pascal. In the inner arc, the sedimentation potential is higher and in the outer arc, due to the positive hydrostatic forces, the erosion potential is higher. Compared to the case without this structure, the negative pressure change in the inner arch is reduced.

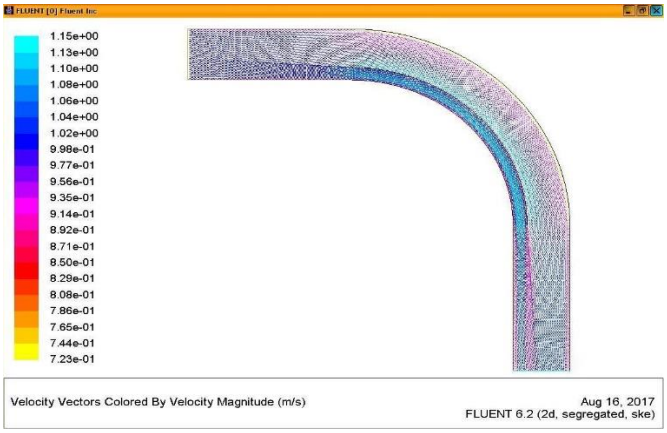

Figure ٨-- Isometric curve, meters per second, in a 90-degree arc with a width of 350 meters and a water height of 4.5 meters. K- ε perturbation model is used. The results show that the velocity values in the inner arc obtained from the numerical model in the presence of the arc vane in a quarter of the width near the inner arc of the beaches immediately after the end of the straight path of the channel and at the beginning of the inner arc, equal to 0.1 m/s and in the arc External is equal to 5.8 meters per second. Compared to the case without this structure, the speed has decreased near the inner arc .The maximum speed was transferred from the inner arc to the middle part. In this way, the amount of negative pressure was reduced and the sedimentation potential was also reduced

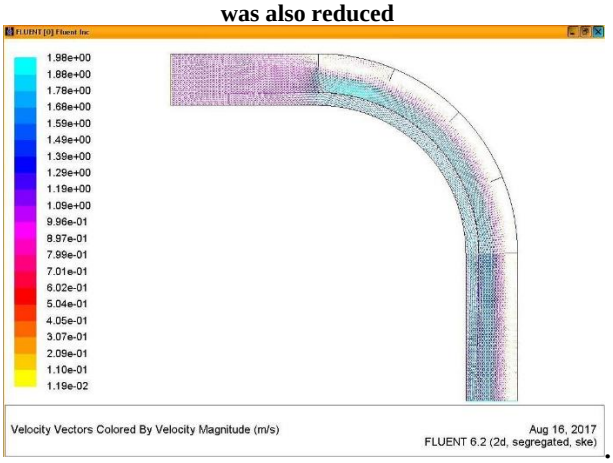

Figure ٩- Isometric curve, meters per second, in an arc of 90 degrees with a width of 350 meters and a water height of 4.5 meters. K- ε perturbation model is used. The results show that the velocity values in the inner arc obtained from the numerical model in the presence of vertical breakwaters in the outer arc along with the arc vane in a quarter of the width near the inner arc of the beaches immediately after the end of the straight path of the channel and at the beginning of the inner arc, equal to ١. ٦٨ m/s and in the outer arc is equal to 7.99 m/s. Compared to the case without this structure, the speed has decreased near the inner arc. The maximum speed was transferred from the inner arc to the middle part. In this way, the amount of negative pressure was reduced and the sedimentation potential was also reduced. Reducing the speed

in the areas between the breakwaters also prevents scouring of this area.

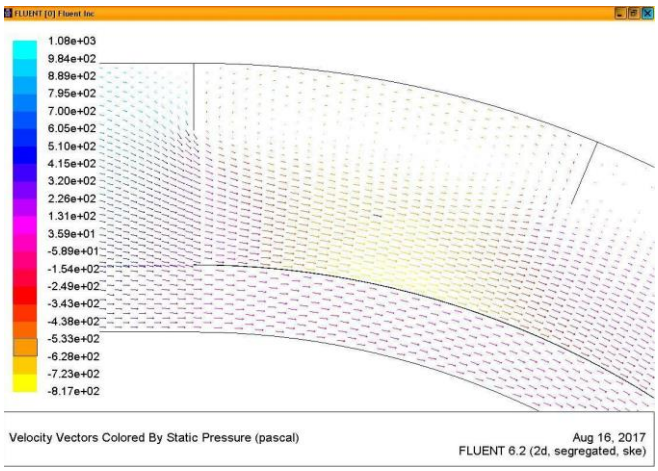

Figure ١٠- isopressure curve in pascal, in a 90 degree arc with a width of 350 meters and a water height of 4.5 meters. K- ε perturbation model is used. The results show that the amount of negative pressure in the outer arch obtained from the numerical model in the presence of vertical breakwaters in the outer arch along with the arch vane between the breakwaters is equal to -8.17e+2 pascals and the positive pressure in the inner arch is equal to 1.31e+2 pascals. Before the construction of protective structures, the potential for sedimentation is higher in the inner arch and the erosion potential is higher in the outer arch due to the positive hydrostatic forces. Compared to the state without these structures, the negative pressure change in the inner arch disappeared and became negative pressure in the outer arch in the space between the breakwaters. In this way, the balance of the navigable river bed was established in the internal and external arcs.

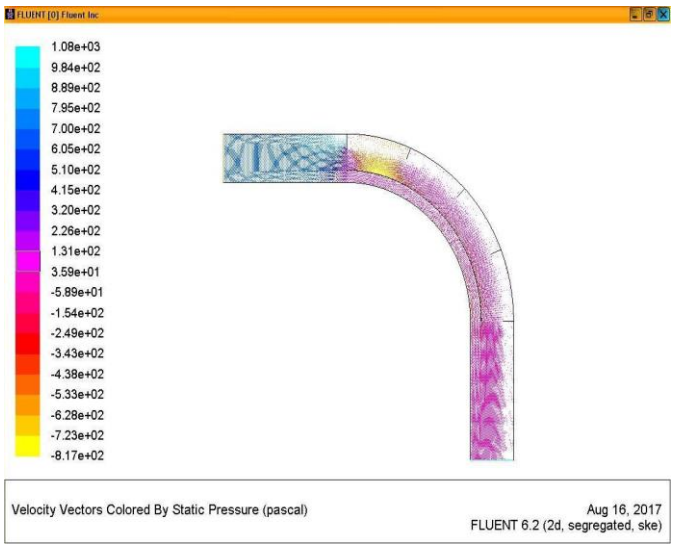

Figure ١١- isopressure curve in pascal, in a 90 degree arc with a width of 350 meters and a water height of 4.5 meters. K- ε perturbation model is used. The results show that the amount of negative pressure in the outer arch obtained from the numerical model in the presence of vertical breakwaters in the outer arch along with the arch vane between the breakwaters is equal to -8.17e+2 pascals and the positive pressure in the inner arch is equal to 1.31e+2 pascals. Before the construction of protective structures, the potential for sedimentation is higher in the inner arch and the erosion potential is higher in the outer arch due to the positive hydrostatic forces. Compared to the state without these structures, the negative pressure change in the inner arch disappeared and became negative pressure in the outer arch in the space between the breakwaters. In this way, the balance of the navigable river bed was established in the internal and external arcs.

5. Conclusions

For the purpose of a case study in the Netherlands, a numerical study of the effect of using submersible vanes along with vertical breakwaters in the protection of the banks of the Waal River in the Netherlands was used from field data. In the present research, the effect of a series of non-submersible breakwaters with 5 placement angles (vertical breakwaters) is numerically investigated, relative to the outer wall of the arch with a length of 25% of the channel width (87.5 meters) and with a distance of 529.875 meters from each other along with a submerged vane in The distance of a quarter of the width from the inner arc to the full length of the 90 degree arc, the distribution of average speed and pressure in the 90 degree arc with a width of 350 meters and a water depth of 4.5 meters was studied. The results of the study showed that the presence of a series of breakwaters causes the uniformity of the upstream speed and the transfer of the high-speed area from the vicinity of the outer wall to the middle of the channel to the inner wall. If the breakwaters are placed in the outer arch along with the submerged blade close to the inner arch at a distance of a quarter of the width, they produce an anti-helix flow which reduces the natural secondary flow in the bends of the river. Therefore, the high-speed current, which is originally pushed towards the inner bank of the bend, is changed and directed to the middle side. Therefore, it will improve sedimentation on the inner shore of the bend and washing water on the outer shore of the bend. In this way, the flow speed reaches from an average value of 1 m/s to a value of 1.98 m/s in the middle part, and sedimentation is reduced in this area, and the potential of sedimentation is reduced by reducing the speed in a quarter of the width near the inner arch. and external increases. According to the results, the speed in the vicinity of the inner shore of the arch is greatly reduced and the placement of breakwaters causes the dispersion and transfer of the high-velocity area from the inner wall to the middle of the channel. The main reason for the sedimentation of the inner coast of the arc is the concentration of areas with negative pressure in the inner arc, which creates a secondary flow and causes a swirling flow and sedimentation in this area. As it can be seen, the placement of the submerged vane with the same length as the arch near the inner arch

along with the breakwaters in the outer arch has prevented the formation of these areas. Due to the speed changes in the vicinity of the breakwaters, the speed has changed and high velocities have been placed at a short distance from the breakwaters. This shows that protecting the nose of breakwaters is inevitable in order to maintain the stability of the breakwater structure.

3. References

1. Qodsian, M.. 2018 final report on scouring, sedimentation and flow pattern around the breakwater in the 90 degree arc. Iran Water Resources Management Joint Stock Company.
2. Tingsanchali, T. and S Maheswaran, 1990. 2-d depth-averaged flow computation near groyne. Journal of Hydraulic Engineering, 116(1): 71-86.
3. Giri, S. Shimizu, Y. and B Surajata, B. 2004. Laboratory measurement and numerical simulation of flow and turbulence in a meandering-like flume with spurs. Flow Measurement and Instrumentation, 15: 301-309.
4. Abad, J. D. and B. L Rhoalds, 2008. Flow structure at different stages in a meander-bend with bend way weirs. Journal of Hydraulic Engineering. 134(8): 1052-1063.
5. Duan, J. He, Li. Fu, X. and Q Wang, 2009. Mean flow and turbulence around experimental spur dike. Advances in Water Resources, 32(12): 1717-1725.
6. Van den Heever, A. 2013. An Investigation of the use of groynes as a means of riverbank erosion protection. M.Sc. Thesis, Department of Civil Engineering, Stellenbosch University, South Africa.
7. Qodsian, M., Waqfi, M. van Panahpour 1387. Laboratory investigation of the two-dimensional flow pattern around the breakwater in a 90 degree arc. Journal of Agricultural Sciences and Natural Resources, 15 (4): 269-282.
8. Fazli, M. Waqfi, M. and Qudsian, M. 2018. Review and comparison of shear stress calculation methods in arched channels. Proceedings of the 8th International Congress of Civil Engineering, Shiraz University, Shiraz.
9. Shaker, A. and Kashfipour, M. 2012. Laboratory investigation of the effect of the length and placement angle of rectangular breakwaters on the distribution of speed and shear stress in a 90 degree arc, Scientific and Research Journal of Irrigation Science and Engineering. Article 1, Volume 38, Number 3.
10. Salehi Nishabouri, S.A.A. and Nasiri Saleh, F, (translators). 2017. Reddy, Wolfgang, (1979), "Disturbance models and their application in hydraulics", Publications of Water Engineering Research School, Tarbiat Modares University, Tehran.
11. Shojaifard, M.J. and Noorpar Hashtroudi, AS (translators). 1379. Versteeg, H.K. and Mallalaskara, (1995), "Introduction to Computational Fluid Dynamics", Iran University of Science and Technology Publications, Tehran.
12. Launder, B. E. and Spalding, D. B. (1974). The Numerical computation of turbulen flows, comput. Methods Appl. Mech. Eng., Vol. 3, pp. 269-289.
13. Tennekes, H, and Lumley, J. L. (1972). A first course in turbulence, MIT Pres Cambridge, MA.
14. Ouillon, S., and Dartus, D. (1997), Three-dimensional computation of flow around groyne, Journal of Hydraulic Engineering, ASCE, 123(11), pp. 962-970.

15. Patankar, S.V. (1980), Numerical heat transfer and fluid flow. Mc Graw- Hill Book Company, New York.
16. Peng, J., Tamai, N., Kawahara, Y., and Huang, G. W. (1999), Numerical modeling of local around spur dikes, 28th IAHR congress, Graz, Austria.
17. Rodi, W. (1984), Turbulence models and their application in hydraulic. State- of- the art paper, IAHR Experimental and Mathematical Fluid Dynamics.
18. Reynolds, O., 1984. On the dynamical theory of incompressible viscous fluids and the determination of the criterion. Phil. Trans. Roy. Soc. London, 123- 161.
19. McGurik, J.J. and Rodi, W., 1978. A depth-averaged mathematical model for the near fluid of side discharge into open- channel flow. Journal of Fluid Mechanics, 864, 761-781.
20. Keller, R.J. and Rodi, W., 1988. Prediction of flow characteristics in main channel/floodplain flows. Journal of Hydraulic Research, IAHR, 26(4), 425- 441.
21. Biglari, B. and Sturm, T.W., 1998. Numerical modeling of flow around bridge abutments in compound channel. Journal of Hydraulic Engineering, ASCE, 124(2), 156-163.
22. Gibson, M.M. and Launder, B.E., 1978. Ground effects on pressure fluctuations in the atmospheric boundary layers. Journal of Fluid Mechanics, 86, 491- 511.
23. Rastogi A. K. and Rodi, W., 1978. Prediction of heat and mass transfer in open channels. Journal of Hydraulics Division, ASCE, 104(3), 397- 420.
24. Yakhot V., Orszag S.A., Thangam, S., Gatski, T.B. and speziale, C.G., 1992. Development of turbulence models for shear flows by a double expansion technique. Physics of Fluids A, Vol. 4, No. 7, pp1510-1520.
25. Wilcox D.C., 1988. Re-assessment of the scale-determining equation for advanced turbulence models. AIAA Journal, vol. 26, pp. 1414- 1421.
26. Versteeg, H.K. and Malalasekera, W., 2007. An Introduction to Computational Fluid Dynamics: The Finite Volume Method, Prentice Hall, Feb 16, 503 pages.
27. Soltani, M.V. and Rahimi Asl, R., 2003. Computational fluid dynamics by Fluent software, Tehran, Tarrah issues.
28. Fluent 6.2 User's Guide, Janurary 2005.
29. Gambit 2.2 User's Guide, September 2004.